Point defects in Ce-doped $Y_3Al_5O_{12}$ crystal scintillators

C. L. Wang,* D. Solodovnikov, and K. G. Lynn
Center for Materials Research, Washington State University, Pullman, Washington 99164-2711, USA
(Received 28 December 2005; revised manuscript received 16 May 2006; published 16 June 2006)

Defect properties of Ce-doped and undoped $Y_3Al_5O_{12}$ (YAG) crystals were studied by Doppler broadening of positron annihilation γ rays and thermoluminescence (TL) as a function of temperature (25–300 °C). The positron diffusion length L_+ was evaluated mainly from the S parameter versus positron energy. Compared with undoped YAG, Ce-doped YAG has a smaller positron diffusion length, due to its higher density of defects. L_+ in Ce-doped YAG decreases with increasing temperature up to 100 °C, and then increases with temperature. The TL intensity in Ce-doped YAG shows the opposite behavior to L_+. The results indicate that point defects probed by positrons may be responsible for the energy transfer to Ce ions and TL intensity. Possible defects detected by positrons are negatively charged or neutral defects related to impurity antisites, cation vacancies, and vacancy complexes.

DOI: 10.1103/PhysRevB.73.233204 PACS number(s): 78.70.Bj

I. INTRODUCTION

Recently there has been intense interest in searching for scintillation materials for radiation detection and medical imaging.[1–3] Optical materials, e.g., halides, oxides, and chalcogenides, were traditionally used as γ-ray and x-ray scintillators.[1] Undoped crystals such as alkali-metal halides were often applied; while metal-ion-doped (such as Ce^{3+}, Eu^{3+}) crystals are more favored as fast scintillators due to their shorter luminescent decay times of 10–100 ns.

Yttrium aluminum garnet ($Y_3Al_5O_{12}$, YAG) doped with rare-earth or transition metals makes excellent laser and optical crystals. Cerium-doped YAG (Ce:YAG) has been used as electron imaging sensors on scanning electron microscopes[4] and radiation scintillators.[5] It was speculated that the luminescence intensity at 550 nm in Ce-doped YAG increases with the concentration of defects such as oxygen vacancies or F centers.[6] These defects also lead to a change in the rise and decay transient profiles of luminescence.[6,7]

Positron annihilation spectroscopy (PAS) is a sensitive method for studying point defects in materials. In this technique, a positron in a solid material is rapidly thermalized and diffuses until it annihilates with an electron, producing two γ quanta that are almost collinear. The energy spectrum of the γ rays is Doppler shifted from 511 keV (the rest mass of electrons), due to momentum conservation in the annihilation processes. If positrons are efficiently trapped at defects such as vacancies and voids, they annihilate with electrons with lower momenta and produce a narrower energy spectrum of γ rays compared with positron annihilation in the bulk. Therefore, the sharpness parameter S can be used to characterize the defects.[8,9] On the other hand, S versus the wing parameter (W) can provide independent information on the number of layers with different defect properties,[10,11] where W is due to positron annihilation with high-momentum electrons (core electrons). Furthermore, the positron energy dependence of S or W can give us the positron diffusion length and therefore information on defect properties in materials.

In this work, defects in cerium-doped YAG were studied by PAS and thermoluminescence (TL). The correlation between TL intensity and defect concentration is discussed. It was shown that controlling defect concentration is crucial for improving luminescence intensity and probably scintillation efficiency.

II. EXPERIMENTS

Three YAG samples grown by the Czochralski (Cz) method were obtained from VLOC (a subsidiary of II-VI, Inc): sample R9 with 0.15 at. % Ce, sample R20 with 1.0 at. % Ce and 1.0 at. % Er, and an undoped YAG sample (R0). Before positron and TL measurements, they were etched in phosphoric acid (85% concentration) at 200 °C to reduce surface damage, and were radiated by a Xe lamp so that the TL intensity was enhanced.[12]

The TL measurement was performed on a heat stage with a heating rate of 12 °C/min after the sample was radiated with a Xe lamp for 15 min. A thermocouple monitored the temperature of heating stage. A photospectrometer (Ocean Optics, Inc.) was used to collect the thermal luminescence. The luminescence spectrum in the region of 500–700 nm shows a peak at around 550 nm. The integrated intensity between 500 and 700 nm was calculated as a function of temperature.

Doppler broadening spectra of positron annihilation γ quanta were measured with a variable-energy positron beam with a flux of about 5×10^5/s cm^2, a diameter of 5 mm, and an energy range of 0.1–12 keV. Thermocouples monitored temperatures at the surface of the sample and the surface and bottom of the heater. Only the temperature on the surface of the samples is used in the positron results. The shape parameters S and W are used in the analysis.[8] As an example, the measured $S(E)$ and $S(W)$ relations[10,11] at room temperature for three samples are shown in Fig. 1.

In Fig. 1(b), the good linear relation between S and W at room temperature indicates that a single layer is adequate to describe the positron behavior,[10] as do the $S(W)$ linear relations at higher temperatures. We used the VEPFIT program[13] to fit $S(E)$ by a single-layer model with an epithermal positron state in the surface. The diffusion lengths had large errors after fixing the bulk S or epithermal parameters at cer-

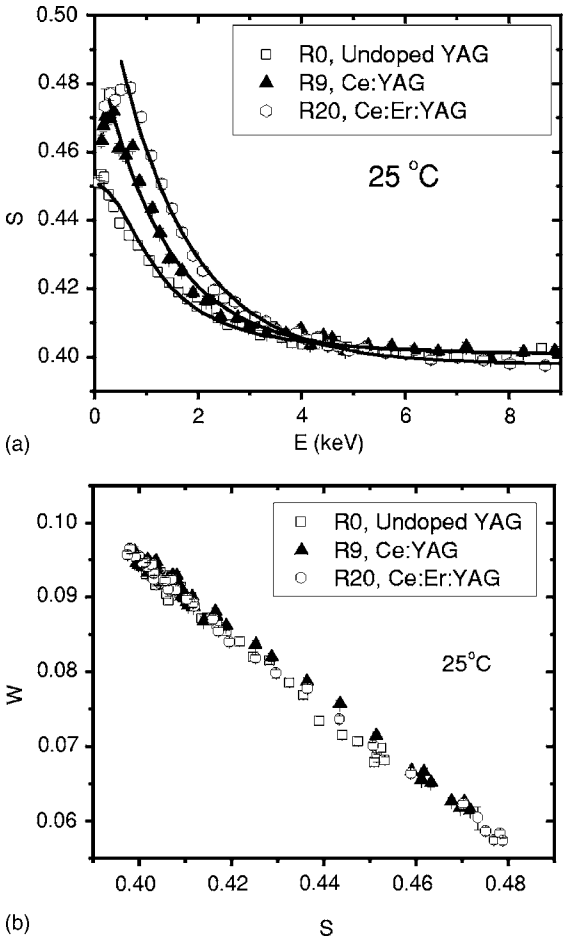

FIG. 1. (a) S parameter as a function of positron energy, (b) S-W relation for three samples at room temperature. Error bars have the same size as the symbols.

tain values (deduced from the first trial fittings), though we could get a good variance of the fit to the experimental $S(E)$ in these trials. To reduce the error bars of the diffusion length, we assumed that the positron implantation profile is a δ function versus positron energy. S versus E is described by $S(E)=S_b+A\exp(-E/E_0)$, where A is the difference between the S values at the surface (S_s) and bulk (S_b), and E_0 is the characteristic energy at which positrons are implanted, thermalized, and diffuse back to the surface with a diffusion length L_+. L_+ is directly calculated based on the mean implantation depth formula $L_+=40E_0^{1.6}/\rho$, where E_0 has units of keV, ρ is the sample density (4.56 g/cm^3), and L_+ is in nanometers.[8] During the fittings of E_0 from $S(E)$ we did not include the small increase of S versus E near the surface for the two Ce-doped samples [Fig. 1(a)], since the charging effect on the Ce-doped YAG surface may increase the positronium (Ps) yield and therefore increases the S values.

The obtained L_+ value may contain a contribution from Ps formed in the surface region. We did not perform the decomposition of the annihilation γ-ray energy spectrum to get the diffusion lengths of Ps and positrons as was done by van Petegem *et al.*,[14] because such a decomposition needs more parameters and the associated errors are supposed to be large. In the bulk YAG crystals, Ps formation is not expected,

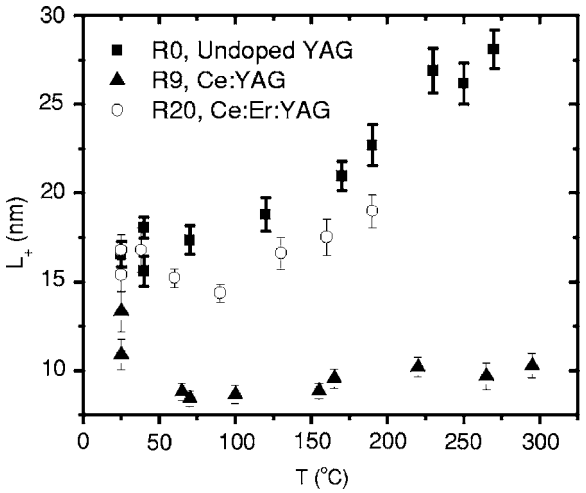

FIG. 2. Positron diffusion length L_+ as a function of temperature for undoped YAG (R0), Ce:YAG (R9), and Er-codoped Ce:YAG samples (R20).

as in other crystalline oxides. We assign L_+ mainly to positron diffusion.

III. RESULTS AND DISCUSSION

The obtained positron diffusion length L_+ is plotted as a function of temperature (Fig. 2). L_+ in the undoped YAG increases with increasing temperature. For the Ce:YAG and Ce:Er:YAG samples, L_+ decreases with increasing temperature up to about 100 °C, and then increases with temperature.

The integrated TL intensities of the two Ce-doped samples are shown in Fig. 3. As an example, the TL profiles at 90 and 110 °C, peaked at around 560 nm, are inset in Fig. 3. This peak is due to the emission of Ce^{3+} ions.[6,7]

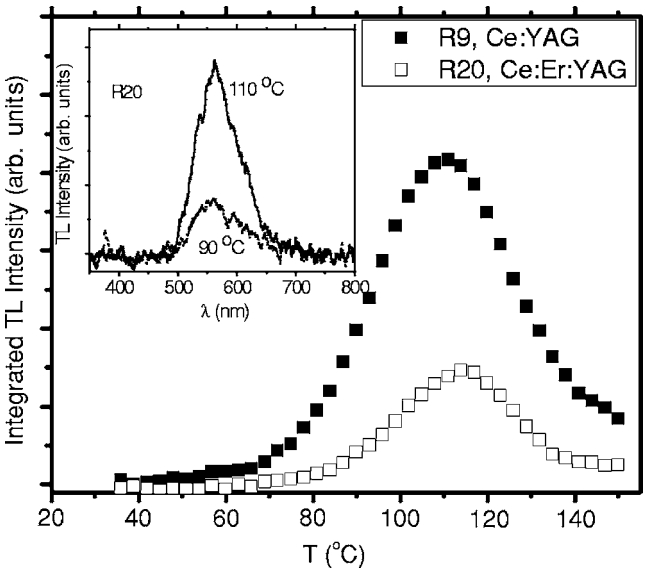

FIG. 3. Thermoluminescence intensity versus temperature for R9 (Ce:YAG) and R20 (Ce:Er:YAG). The inset shows TL spectra at 90 and 110 °C for sample R20.

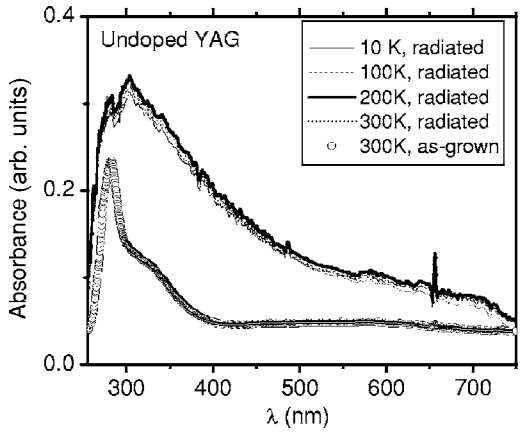

FIG. 4. Optical absorption spectrum of undoped YAG sample under UV radiation (curves) as a function of temperature. As a comparison, the spectrum of as-grown undoped YAG sample (circles) at 300 K is also shown.

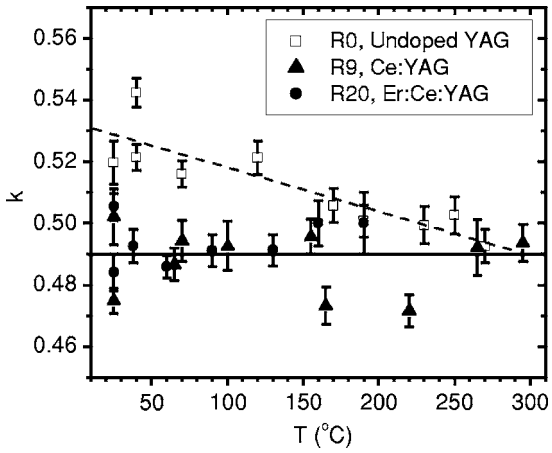

FIG. 5. Slope k of S-W curve as a function of temperature for undoped, Ce:YAG, and Ce:Er:YAG samples. Dashed and solid lines indicate the tendency of k versus temperature for undoped YAG and the two Ce-doped YAG samples, respectively.

Undoped crystalline YAG has a smaller positron diffusion length L_+ (15–30 nm), compared with other Cz-grown crystals such as Si (L_+=230 nm).[9] Furthermore, L_+ in undoped YAG increases with temperature, in contrast with the decrease of L_+ with increasing temperature for many crystalline materials.[8] We attribute these observations to the various amounts of metal impurities in a typical YAG crystal with concentrations of 1–100 ppm as measured by glow discharge mass spectroscopy. Metal impurities can easily form color centers by combination with oxygen atoms and trapped charges.[7,15]

The optical absorption spectrum of the undoped YAG sample R0 under UV radiation was measured as a function of temperature (10–300 K) (Fig. 4). The absorption spectrum has peaks at ~300 and ~580 nm with a long tail up to 750 nm. Compared with as-grown undoped YAG, the sample under UV radiation has larger absorption coefficients at 300 K, indicating higher defect concentrations. No systematic change in absorption spectrum was observed as a function of temperature for the UV-irradiated sample. The broad optical absorption spectra of YAG cannot be assigned to a single defect center. These defects probably are deeply located at 2.1–4.2 eV from the valence band (VB) in the wide band gap (~6.5–7.0 eV) of YAG.[16,17] Most of defects are located at ~4.2 eV above the VB, or about 0.9 eV above the Fermi energy level of YAG. Defects or color centers in Ce:YAG were also confirmed by light absorption, photoluminescence (PL), and PL excitation spectra.[6]

Now let us consider the difference in positron diffusion length L_+ in the three tested samples using a simple picture. Based on the two-state trapping model, L_+ is related to the defect concentration n_t as follows:[9]

$$L_+ = \left(\frac{D_+}{k_t n_t + \lambda_b} \right)^{1/2}, \qquad (1)$$

where λ_b is the positron annihilation rate in the bulk, D_+ is the positron diffusion constant, and k_t is the rate constant of positron trapping in the defects and is assumed to be the same for doped and undoped YAG samples as long as the defect type is the same.[6] Assuming λ_b is the same for all three samples, a smaller L_+ indicates a larger defect concentration through the explicit relationship in Eq. (1) and the implicit relationship that D_+ is decreased with the increase of defect concentration n_t due to more frequent scatterings off defects or impurities.[18]

Noticeably the L_+ values in Ce:Er:YAG, almost the same as those in undoped YAG, are larger than those in Ce:YAG (Fig. 2). Possibly Er ions reduce the concentration of defects in Ce:YAG. This is not surprising since 50 at. % Er can be doped in YAG during crystal growth, resulting in an excellent laser crystal in IR emission.[19]

The S parameter in the bulk (S_b) was usually regarded as a defect indicator for Si-based semiconductor materials such as c-Si, a-Si, SiO_2, and also for some metals.[8,9] In our samples, we did not observe a clear correlation between S_b and L_+ or a systematic variation of S_b with temperature. Different kinds of impurities and defects are expected to have complicated influences on the positron trapping and scattering and therefore on S_b values. L_+ rather than S_b might be a good indicator of overall crystal qualities.

It is interesting to plot the slope $k=dW/ds$ of the S-W curve versus temperature. The results are shown in Fig. 5. The slope k is characteristic of the defects where positrons are localized and annihilated.[11] If k is a constant versus temperature, it means the type of defect does not change with temperature, regardless of the variation of defect concentration with temperature. For undoped YAG, k tends to decrease with increasing temperature within experimental errors, possibly due to the transformation of defect types at temperatures of 25–270 °C. On the contrary, k is a constant (0.49±0.01) versus temperature within experimental errors for the two Ce-doped YAG samples, suggesting that Ce^{3+} ions play an important role in determining the type and temperature stability of positron-sensitive defects.

The thermoluminescence intensity has a peak at the transition point T_{TL}=110–115 °C for Ce:YAG and Ce:Er:YAG samples (Fig. 3). T_{TL} is about 10 °C higher than the charac-

teristic temperature $T_P = 100\ ^\circ C$ at which the positron diffusion length reaches a minimum. There is a temperature gradient along the depth of the YAG samples due to the low thermal conductivity of YAG. T_P is measured near the surface of the sample, while T_{TL} is the average temperature in the bulk. Within this small difference in transition temperatures, we can safely say that the TL intensity increases concomitantly with the increase in concentration of defects probed by positrons.

Robbins *et al.* proposed that energy trapped at defect centers in Ce:YAG can be thermally released and might be transferred to Ce^{3+} ions directly by long-range resonance transfer, or indirectly by thermal release of excitation energy from the excited defect centers into delocalized lattice states when retrapping at an activator site becomes possible.[7,20] YAG is a crystal with a wide optical band gap of 6.5–7.0 eV. The relative position of the Ce^{3+} excited $5d$ level is $\sim$1.5 eV below the conduction band (CB) edge in YAG,[17] and the $4f$ ground level is about 2.5 eV above the valence band edge.[16] Defects with energy levels located at 4.1 eV above the VB may have a probability of transferring the energy to the Ce^{3+} $4f$ ground level, depending on the defect- Ce^{3+} distance and temperature. Our result indicates that neutral or negatively charged defects in Ce-doped YAG samples, as probed by positrons, may be helpful for energy transfer to the Ce^{3+} ground state and an increase in luminescence intensity emitted from Ce^{3+}. In addition, Er^{3+} codoping in Ce:YAG reduces the defect concentration compared with Ce:YAG (Fig. 2), and therefore reduces TL intensity.

Kuklja[21] calculated the formation energies of impurity-induced or intrinsic defects in YAG using a pair-potential approximation coupled with a shell model. It was concluded that the most stable negatively charged and neutral defects in YAG are (i) a divalent antisite on Y^{3+} compensated by an oxygen vacancy; (ii) two divalent antisites combined with an oxygen vacancy; (iii) trivalent impurities on Al^{3+} or Y^{3+}, which form neutral defects and possibly provide potential wells to trap positrons; (iv) the negatively charged cation vacancies created simultaneously with the tetravalent impurity antisites on Al^{3+}. These defects are the possible trapping sites for positrons. The relative contributions of these defects to positron trapping and TL intensity, probably dependent on the impurity concentrations, call for additional studies in future.

IV. CONCLUSION

Positron annihilation and thermoluminescence spectra versus temperature (25–300 °C) have been measured for undoped YAG, Ce:YAG, and Ce:Er:YAG. A good correlation between positron diffusion length and TL intensity versus temperature was found in a qualitative sense. It indicates that neutral or negatively charged defects, located deep in the band gap of YAG, may help the energy transfer to Ce^{3+} ions and enhance TL. It is reasonable to claim that controlling the defect concentration and making energy transfer more efficient are important for phosphor optimization. We speculate that transparent Ce-doped polycrystalline (or ceramic[3]) and nanocrystalline YAG might be good candidates for efficient scintillators, since their growth temperatures are lower and they may have a more efficient energy transfer from defects to Ce ions compared with single-crystal YAG. Combined with positron annihilation Doppler broadening measurements, positron lifetimes in YAG samples will provide more quantitative information on positron trapping rates in defects and defect concentrations.

We acknowledge DOE Basic Energy Sciences (Contract No. ER 46103) for supporting this work. We also thank Tia Buchanan for crystal growth, and M. Weber, C. Shawley, and S. McNeil for their help in experiments and discussion.

*Email address: cai-lin.wang@parttec.com

[1] P. A. Rodnyi, *Physical Processes in Inorganic Scintillators* (CRC, Boca Raton, FL, 1997).
[2] C. W. E. van Eijk, Phys. Med. Biol. **47**, R85 (2002).
[3] C. Greskovich and S. Duclos, Annu. Rev. Mater. Sci. **27**, 69 (1997).
[4] P. Autrata, P. Schauer, J. Kvapil, and J. Kvapil, J. Phys. E **11**, 707 (1978).
[5] M. Moszynski, T. Ludziejewski, D. Wolski, W. Klamra, and L. O. Norlin, Nucl. Instrum. Methods Phys. Res. A **345**, 461 (1994).
[6] C. M. Wong, S. R. Rotman, and C. Warde, Appl. Phys. Lett. **44**, 1038 (1984).
[7] D. J. Robbins, B. Cockayne, B. Lent, C. N. Duckworth., and J. L. Glasper, Phys. Rev. B **19**, 1254 (1979).
[8] P. J. Schultz and K. G. Lynn, Rev. Mod. Phys. **60**, 701 (1988).
[9] P. Asoka-Kumar, K. G. Lynn, and D. O. Welch, J. Appl. Phys. **76**, 4935 (1994).
[10] M. Clement, J. M. M. de Nijs, P. Balk, H. Schut, and A. van Veen, J. Appl. Phys. **79**, 9029 (1996).
[11] L. Liszkay, C. Corbel, L. Baroux, P. Hautojarvi, M. Bayhan, A. W. Brinkman, and S. Tatarenko, Appl. Phys. Lett. **64**, 1380 (1994).
[12] A. Vedda, M. Martini, F. Meinardi, J. Chval, M. Dusek, J. A. Mares, E. Mihokova, and M. Nikl, Phys. Rev. B **61**, 8081 (2000).
[13] A. van Veen, H. Schut, J. de Vries, R. A. Hakvoort, and M. R. IJpma, in *Positron Beams for Solids and Surfaces*, edited by P. J. Schultz, G. R. Massoumi, and P. J. Simpson (AIP, New York, 1991).
[14] S. van Petegem, C. Dauwe, T. van Hoeke, J. de Baerdemaeker, and D. Segers, Phys. Rev. B **70**, 115410 (2004).
[15] O. F. Schirmer, K. W. Blazey, W. Berlinger, and K. Diehl, Phys. Rev. B **11**, 4201 (1975).
[16] C. W. Thiel, H. Cruguel, H. Wu, Y. Sun, G. J. Lapeyre, R. L. Cone, R. W. Equall, and R. M. Macfarlane, Phys. Rev. B **64**, 085107 (2001).
[17] E. Zych, C. Brecher, and J. Glodo, J. Phys.: Condens. Matter **12**, 1947 (2000).
[18] M. J. Puska and R. M. Nieminen, Rev. Mod. Phys. **66**, 841 (1994).
[19] W. Koechner, *Solid-State Laser Engineering*, 5th ed. (Springer, Berlin, 1999).
[20] D. J. Robbins and P. J. Dean, Adv. Phys. **27**, 499 (1978).
[21] M. M. Kuklja, J. Phys.: Condens. Matter **12**, 2953 (2000).